ISSN (Print) 1226-1750
ISSN (Online) 2233-6656
Journal of Magnetics 26(3), 285-293 (2021) https://doi.org/10.4283/JMAG.2021.26.3.285

Implication of Magneto-hydrodynamics and Melting Heat Transfer in Cubic Autocatalytic Reactive Flow with Entropy Generation

Sohail A. Khan[1], M. Ijaz Khan[2]*, Sami Ullah Khan[3], M. Y. Malik[4], and A. Ghareeb[5,6]

[1]*Department of Mathematics, Quaid-I-Azam University 45320, Islamabad 44000, Pakistan*
[2]*Department of Mathematics and Statistics, Riphah International University I-14, Islamabad 44000, Pakistan*
[3]*Department of Mathematics, COMSATS University Islamabad, Sahiwal, 57000, Pakistan*
[4]*Department of Mathematics, College of Sciences, King Khalid University, Abha, 61413, Saudi Arabia*
[5]*Department of Mathematics, College of Science, Al-Baha University, Al-Baha 65799, Saudi Arabia*
[6]*Department of Mathematics, Faculty of Science, South Valley University, Qena 83523, Egypt*

(Received 23 June 2021, Received in final form 29 September 2021, Accepted 29 September 2021)

The theme of this article is to investigate hydrodynamic flow of an incompressible second grade nanoliquid by a curved stretched sheet. Energy expression is developed through dissipation and Joule heating. Brownian and thermophoresis diffusion are also scrutinized. Physical feature of entropy generation is discussed. Isothermal cubic autocatalytic chemical reactions are discussed. Suitable transformations are used to develop the ordinary differential system. To develop a convergent series solution we employed the Optimal Homotopy Analysis Technique (OHAM). Graphical description of velocity, entropy generation, temperature distribution and concentration versus sundry parameters are discussed. An opposite behavior in velocity field is noted for magnetic and curvature parameters. Temperature distribution and velocity field have reverse trends for melting parameter. An augmentation in temperature is observed for radiation parameter. Larger magnetic variable lead to improve the entropy generation. Entropy optimization is boosted versus higher magnetic parameter.

Keywords : second grade fluid, curved stretching surface, melting heat, thermal radiation, thermophoresis, entropy generation, cubic autocatalytic chemical reactions and brownian diffusion

1. Introduction

Thermal energy is sum of potential and kinetic energies of particles that make up a material. Thermal energy is stored as a result of change in interior energy of the material such as reaction heat, latent heat, sensible heat or the combination of all of these. The heat which exchanges the materials with environment during the phase change is known as latent heat. Heat energy is stored in phase change materials (PCM) in latent heat form. Phase change materials (PCM) fluctuates its phase as its interior heat changes efficiently. Non-Newtonian liquids flow with melting heat communication have tremendous applications in innovative thermal engineering such as optimal utilization of energy, magma solidification, welding processes, solar energy systems, latent heat thermal energy storage, thermal insulation, production of semiconductors, permafrost thermal protection melting, geothermal energy recovery and many others. With the intention of thermal energy storage the materials with high latent heat are responsible to phase changes at constant temperature. Furthermore the constant temperature characteristics during phase change is also used to afford temperature control which having most significant in thermal management and electronic cooling phenomena [1]. It is obvious that the thermal transportation characteristics are very significant in defining the thermo-fluidic performance of an isolated thermal system with phase change materials (PCM) as the heat transfer and energy storage. Due to this fact heat discharging and charging are recognized. Melting heat transfer analysis in a semi-infinite piece of ice located in a hot stream of air is analyzed by Robert [2]. Mabood and Mastroberardino [3] studied the melting effect in magnetohydrodynamic nanoliquid flow towards a stretching sheet with slip and dissipation effects. Numerical analysis of melting heat in fluid flow is

*Corresponding author: Tel: +92-335-9761475
Fax: +92-335-9761475, e-mail: ijazfmg_khan@yahoo.com

illustrated by Gurel [4]. Hayat *et al.* [5] studied melting heat effect in dissipative flow of hybrid nanoliquid towards stretched sheet. Melting effect in reactive flow of Williamson nanoliquid toward porous stretchable medium with radiation is analyzed by Krishnamurthy *et al.* [6]. Sheikholeslami and Rokni [7] reported the melting heat influence in convective flow of nanoliquid flow with Lorentz force inside cavity. Some advancements about heat transfer aspects are highlighted in Refs. [8-20].

Nanomaterials have innovative properties such as minimal clogging in flow passages, homogeneity high thermal conductivity and long-term stability. It is because of large surface areas and small size of nanoparticles. Nanoliquids are the combination of nano-zise (1-100 nm) solid particles and traditional exploitable liquids. By insertion of nano-zise particles we improve thermal conduction performance of traditionally utilizable liquids (like air, water, ethylene glycol and mineral). Nanomaterials have tremendous applications in heat exchangers, electronics cooling, food processing, pharmacological administration mechanisms, solar collectors, micro-manufacturing, peristaltic pumps for diabetic treatments, heat pumps, chemical industries and nuclear applications etc. Initially Choi [21, 22] gave the concept of nanomaterials for augmentation of thermal conduction performance of traditional exploitable liquids by using nanoliquids. Buongiorno [23] has accomplished innovative work on nanoliquids thermal conductivity enhancement. Some relevant studies about nanomaterial flow is presented in Refs. [24-31].

Entropy optimization is employed to demonstrate the performance of numerous closed systems in manufacturing, refrigerators, engineering and industrial processes. Entropy is produced in any irreversible phenomena such as viscosity of the fluid, diffusion, thermal resistance to the liquid flow, heat flux, friction of solid surfaces, chemical reactions, molecules vibration, Joule heating and many others. Entropy optimization is used to enhance the performance of any closed thermal system. Irreversibility analysis in convective flow with thermal transportation is discussed by Bejan [32, 33]. Hayat *et al.* [34] analyzed irreversibility in dissipative flow of Ree-Eyring nanoliquid with Brownian and thermophoresis diffusions between rotating disks. Some relevant studies about Newtonian and non-Newtonian materials can be seen in Refs. [35-45].

Theme of this article is to analyze irreversibility analysis in MHD flow of second grade nanoliquid by a curved stretching surface. Combined effect of radiation, Brownian diffusion, radiation and thermophoresis are discussed in heat equation. Melting effect is also accounted. Irreversibility analysis is modeled through thermodynamics second law. Isothermal quartic autocatalytic reactions are discussed. Ordinary differential system are obtained through transformation procedure. For convergent solution we used OHAM [46-50]. Influences of different flow variables on velocity, temperature, entropy rate and concentration are graphically analyzed.

2. Statement

Here steady magnetohydrodynamic flow of an incompressible second grade nanofluid by a curved stretched surface is considered. Joule heating and dissipation effects are addressed in energy expression. Melting effect is discussed. Furthermore Brownian and thermophoresis diffusions are scrutinized. Description of irreversibility is also accounted. Isothermal cubic autocatalytic reactions are discussed. Governing equation is modeled through curvilinear coordinates (r, s). Consider $u_w = as$ as the stretching velocity with positive rate constant (a). Constant magnetic force of strength (B_0) is exerted. Physical flow diagram is highlighted in Fig. 1.

Isothermal cubic autocatalytic reaction is satisfied by [51-54]:

$$A + 2B \to 3B, \qquad \text{with reaction rate} = k_1^* C_2 C_2^3, \tag{1}$$

Isothermal first order chemical reaction satisfies

$$A \to B, \qquad \text{with reaction rate} = k_2^* C_2 \tag{2}$$

After applying the boundary layer approximations we have [55-57]:

$$(r+R)\frac{\partial v}{\partial r} + v + R\frac{\partial u}{\partial s} = 0, \tag{3}$$

$$\frac{u^2}{r+R} + \frac{1}{\rho_f}\frac{\partial p}{\partial r} = 0, \tag{4}$$

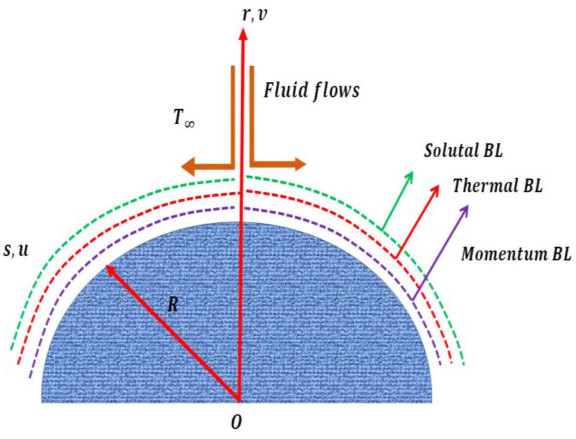

Fig. 1. (Color online) Flow diagram.

$$\left.\begin{aligned} v\frac{\partial u}{\partial r}+\frac{uR}{r+R}\frac{\partial u}{\partial s}+\frac{uv}{r+R}=-\frac{1}{\rho_f}\frac{R}{r+R}\frac{\partial p}{\partial s}+\nu_f\left(\frac{\partial^2 u}{\partial r^2}+\frac{1}{(r+R)}\frac{\partial u}{\partial r}-\frac{u}{(r+R)^2}\right)\\ +\frac{\alpha_1^*}{\rho_f}\left(\begin{array}{l}\frac{2R}{(r+R)}\frac{\partial^2 u}{\partial r^2}\frac{\partial u}{\partial s}-\frac{2R}{(r+R)^2}\frac{\partial u}{\partial r}\frac{\partial u}{\partial s}+\frac{2}{(r+R)}\frac{\partial v}{\partial r}\frac{\partial u}{\partial r}+\frac{2}{(r+R)}v\frac{\partial^2 u}{\partial r^2}\\ -\frac{2}{(r+R)}v\frac{\partial u}{\partial r}-\frac{4R}{(r+R)^2}u\frac{\partial^2 u}{\partial r\partial s}-\frac{4R}{(r+R)^2}u\frac{\partial v}{\partial r}+\frac{2R}{(r+R)^3}u\frac{\partial u}{\partial s}\end{array}\right)-\frac{\sigma_f}{\rho_f}B_0^2u\end{aligned}\right\}, \tag{5}$$

$$\left.\begin{aligned} v\frac{\partial T}{\partial r}+\frac{uR}{r+R}\frac{\partial T}{\partial s}=\left(\frac{k}{(\rho c_p)_f}+\frac{16\sigma^* T_\infty^3}{3k^*(\rho c_p)_f}\right)\left(\frac{1}{r+R}\frac{\partial T}{\partial r}+\frac{\partial^2 T}{\partial r^2}\right)+\frac{\sigma_f}{\rho_f}B_0^2u^2\\ +\tau\left(D_{C_1}\frac{\partial C_1}{\partial r}\frac{\partial T}{\partial r}+\frac{D_T}{T_\infty}\left(\frac{\partial T}{\partial r}\right)^2+D_{C_2}\frac{\partial C_2}{\partial r}\frac{\partial T}{\partial r}\right)\end{aligned}\right\}, \tag{6}$$

$$\begin{aligned} v\frac{\partial C_1}{\partial r}+\frac{uR}{r+R}\frac{\partial C_1}{\partial s}=D_{C_1}\left(\frac{1}{r+R}\frac{\partial C_1}{\partial r}+\frac{\partial^2 C_1}{\partial r^2}\right)\\ +\frac{D_T}{T_\infty}\left(\frac{1}{r+R}\frac{\partial T}{\partial r}+\frac{\partial^2 T}{\partial r^2}\right)-k_1^*C_1C_2^3,\end{aligned} \tag{7}$$

$$\begin{aligned} v\frac{\partial C_2}{\partial r}+\frac{uR}{r+R}\frac{\partial C_2}{\partial s}=D_{C_2}\left(\frac{1}{r+R}\frac{\partial C_2}{\partial r}+\frac{\partial^2 C_2}{\partial r^2}\right)\\ +\frac{D_T}{T_\infty}\left(\frac{1}{r+R}\frac{\partial T}{\partial r}+\frac{\partial^2 T}{\partial r^2}\right)+k_1^*C_1C_2^3,\end{aligned} \tag{8}$$

$$\left.\begin{aligned} u=as,\ T=T_m,\ D_{C_1}\frac{\partial C_1}{\partial r}=-D_{C_2}\frac{\partial C_2}{\partial r}=k_2^*C_1 \text{ at } r=0,\\ u\to 0,\ \frac{\partial u}{\partial r}\to 0,\ T\to T_\infty,\ C_1\to C_0,\ C_2\to 0 \text{ as } r\to\infty.\\ k_f\left(\frac{\partial T}{\partial r}\right)=\rho_f\left[\lambda+C_s\left(T_m-T_0\right)\right]v(s,0)\end{aligned}\right\}. \tag{9}$$

By using

$$\left.\begin{aligned} u=asf'(\eta),\ v=-\frac{R}{r+R}\sqrt{a\nu_f}f(\eta),\ p=\rho_f a^2s^2P(\eta),\\ \theta(\eta)=\frac{T-T_m}{T_\infty-T_m},\ \phi(\eta)=\frac{C_1}{C_0},\ l(\eta)=\frac{C_2}{C_0},\ \eta=\sqrt{\frac{a}{\nu_f}}r,\end{aligned}\right\}, \tag{10}$$

we have

$$P'-\frac{f'^2}{(\eta+A)}=0, \tag{11}$$

$$\left.\begin{aligned} \frac{2A}{(\eta+A)}P=f'''+\frac{1}{(\eta+A)}f''-\frac{1}{(\eta+A)^2}f'+\frac{A}{(\eta+A)}ff''+\frac{A}{(\eta+A)^2}ff'-\frac{A}{(\eta+A)}f'^2\\ \beta\left(\frac{2A}{(\eta+A)}ff'''-\frac{2A}{(\eta+A)^2}ff''-\frac{8A}{(\eta+A)^2}ff''+\frac{4A}{(\eta+A)^3}ff''+\frac{6A}{(\eta+A)^3}f'^2-\frac{4A}{(\eta+A)^4}ff'\right)-Mf',\end{aligned}\right\}, \tag{12}$$

$$\left(1+Rd\right)\left(\theta''+\frac{1}{(\eta+A)}\theta'\right)+\Pr\frac{A}{(\eta+A)}f\theta'+\Pr Nt\theta'^2 +M\Pr Ecf'^2=0, \tag{13}$$

$$\frac{1}{Sc}\left(\phi''+\frac{1}{(\eta+A)}\phi'\right)+\frac{A}{(\eta+A)}f\phi' +\frac{1}{Sc}\frac{Nt}{Nb}\left(\theta''+\frac{1}{(\eta+A)}\theta'\right)-K_1\phi l^3=0, \tag{14}$$

$$\begin{aligned} \frac{\delta}{Sc}\left(l''+\frac{1}{(\eta+A)}l'\right)+\frac{A}{(\eta+A)}fl'\\ +\frac{1}{Sc}\frac{Nt}{Nb}\left(\theta''+\frac{1}{(\eta+A)}\theta'\right)+K_1\phi l^3=0,\end{aligned} \tag{15}$$

with

$$\left.\begin{aligned} f'(\eta)=1,\ \theta(\eta)=0,\ \ \Pr f(\eta)+Me\theta'(\eta)=0,\\ \phi'(\eta)=K_2\phi(\eta),\ \ \delta l'(\eta)=-K_2\phi(\eta)\ \ \text{at } \eta=0\\ f'(\infty)=0,\ f''(\infty)=0,\ \ \theta(\infty)=1,\ \ \phi(\infty)=1,\ \ l(\infty)=0.\end{aligned}\right\}. \tag{16}$$

Dimensionless variables are

$$\left.\begin{aligned} M=\frac{\sigma_f B_0^2}{a\rho_f},\ \beta=\frac{\alpha_1^* a}{\mu_f},\ \ A=\sqrt{\frac{a}{\nu_f}}R,\ Rd=\frac{16\sigma^* T_\infty^3}{3k^*k_f},\\ Nt=\frac{\tau D_T(T_\infty-T_m)}{T_\infty\nu_f},\ \ \Pr=\frac{\nu_f}{\alpha},\ Nb=\frac{\tau D_B C_0}{\nu_f},\ \ Ec=\frac{u_w^2}{c_p(T_\infty-T_m)},\\ Me=\frac{(c_p)_f(T_\infty-T_m)}{\lambda+C_s(T_m-T_0)},\ Sc=\frac{\nu_f}{D_{C_1}},\ K_1=\frac{k_1^*C_0^3}{a},\ K_2=\frac{k_2^*}{D_{C_1}}\sqrt{\frac{a}{\nu_f}},\ \delta=\frac{D_{C_2}}{D_{C_1}}\end{aligned}\right\}. \tag{17}$$

By neglecting the pressure we have

$$\left.\begin{aligned} f^{iv}+\frac{2}{(\eta+A)}f'''-\frac{1}{(\eta+A)^2}f''+\frac{1}{(\eta+A)^3}f'+\frac{A}{(\eta+A)}\left(ff'''-f'f''\right)\\ +\frac{A}{(\eta+A)^2}\left(ff''-f'^2\right)-\frac{A}{(\eta+A)^3}ff'\\ +2\beta\left(\begin{array}{l}\frac{A}{(\eta+A)}f'f'''+\frac{A}{(\eta+A)}ff^{iv}+\frac{3A}{(\eta+A)^3}ff'''-\frac{5A}{(\eta+A)^2}ff'''-\frac{A}{(\eta+A)^2}ff^{iv}\\ +\frac{12A}{(\eta+A)^3}ff''-\frac{4A}{(\eta+A)^2}f''^2-\frac{6A}{(\eta+A)^4}ff''-\frac{8A}{(\eta+A)^4}f'^2+\frac{6A}{(\eta+A)^5}ff'\end{array}\right)\\ -M\left(f''+\frac{1}{(\eta+A)}f'\right)=0\end{aligned}\right\}. \tag{18}$$

For same diffusion coefficient $D_{C_1}=D_{C_2}$ we have

$$\phi(\eta)+l(\eta)=1 \tag{19}$$

From Eqs. (14) and (15) we have

$$\begin{aligned} \frac{1}{Sc}\left(\phi''+\frac{1}{(\eta+A)}\phi'\right)+\frac{A}{(\eta+A)}f\phi'\\ +\frac{1}{Sc}\frac{Nt}{Nb}\left(\theta''+\frac{1}{(\eta+A)}\theta'\right)-K_1\phi(1-\phi)^3=0\end{aligned} \tag{20}$$

$$\phi'(\eta)=K_2\phi(\eta),\quad \phi(\infty)=1. \tag{21}$$

3. Engineering Quantities

3.1. Surface drag force

It is expressed by

$$C_{fs}=\frac{\tau_{rs}}{\frac{1}{2}\rho_f u_w^2}, \tag{22}$$

with τ_{rs} as shear stress satisfying

$$\tau_{rs}=\mu_f\left(\frac{\partial u}{\partial r}-\frac{u}{r+R}\right)+2\alpha\left(\begin{array}{c}\frac{R}{r+R}\frac{\partial u}{\partial r}\frac{\partial u}{\partial s}+\frac{v}{r+R}\frac{\partial u}{\partial r}\\ -\frac{2Ru}{(r+R)^2}\frac{\partial u}{\partial s}-\frac{2uv}{(r+R)^2}\end{array}\right)\Bigg|_{r=0}, \quad (23)$$

Finally we have

$$C_{fs}\,\mathrm{Re}_s^{1/2}=2\left[f''(0)-\frac{f'(0)}{A}+\beta\left(f'(0)f''(0)-\frac{2}{A}\left(f'(0)^2\right)\right)\right]. \quad (24)$$

3.2. Nusselt number

It is defined as

$$Nu_s=\frac{sq_w}{k_f\left(T_\infty-T_m\right)}, \quad (25)$$

with heat flux q_w satisfies

$$q_w=-k_f\left(1+\frac{16\sigma^*T_\infty^3}{3k^*k_f}\right), \quad (26)$$

We have

$$Nu_s\,\mathrm{Re}_s^{-1/2}=-(1+Rd)\theta'(0). \quad (27)$$

4. Entropy Generation

Mathematically

$$S_G=\left.\begin{array}{c}\frac{k_f}{T_\infty^2}\left(1+\frac{16\sigma^*T_\infty^3}{3k^*k_f}\right)\left(\frac{\partial T}{\partial r}\right)^2+\frac{\sigma_f B_0^2}{T_\infty}u^2+\frac{R_{D_{C_1}}}{T_\infty}\left(\frac{\partial T}{\partial r}\frac{\partial C_1}{\partial r}\right)\\ +\frac{R_{D_{C_1}}}{C_1}\left(\frac{\partial C_1}{\partial r}\right)^2\frac{R_{D_{C_2}}}{T_\infty}\left(\frac{\partial T}{\partial r}\frac{\partial C_2}{\partial r}\right)+\frac{R_{D_{C_2}}}{C_2}\left(\frac{\partial C_2}{\partial r}\right)^2\end{array}\right\}, \quad (28)$$

One can write

$$\left.\begin{array}{c}N_G(\eta)=\alpha_{11}(1+Rd)\theta'^2+MBrf'^2\\ +\frac{\phi'^2}{\alpha_1}\left(\frac{L_1}{\varphi}+\frac{L_2}{(1-\varphi)}\right)+(L_1-L_2)\theta'\phi'.\end{array}\right. \quad (29)$$

Dimensionless parameters are

$$\left.\begin{array}{c}S_G=\frac{S_GT_\infty v_f}{ak_f(T_\infty-T_m)},\ \alpha_1=\frac{T_\infty-T_m}{T_\infty},\ Br=\frac{\mu_f u_w^2}{k_f(T_\infty-T_m)}\\ L_1=\frac{R_{D_{C_1}}C_0}{k_f},\ L_2=\frac{R_{D_{C_2}}C_0}{k_f}\end{array}\right\}. \quad (30)$$

5. Solution Methodology

To construct series solution we implemented the OHAM [46, 47]. Initial guesses and linear operators are

$$\left.\begin{array}{c}f_0(\eta)=\left(e^{-\eta}-e^{-2\eta}\right)-\frac{Me}{\mathrm{Pr}}\\ \theta_0(\eta)=1-e^{-\eta}\\ \phi_0(\eta)=1-e^{-K_2\eta}\end{array}\right\}, \quad (31)$$

$$\left.\begin{array}{c}L_f=\frac{\partial^4}{\partial\eta^4}-5\frac{\partial^2}{\partial\eta^2}+4\\ L_\theta=\frac{\partial^2}{\partial\eta^2}-1\\ L_\phi=\frac{\partial^2}{\partial\eta^2}-1\end{array}\right\}, \quad (32)$$

with

$$\left.\begin{array}{c}L_f\left[z_1e^{\eta}+z_2e^{-\eta}+z_3e^{2\eta}+z_4e^{-2\eta}\right],\ L_\theta\left[z_5e^{\eta}+z_6e^{-\eta}\right]\\ L_\phi\left[z_7e^{\eta}+z_8e^{-\eta}\right]\end{array}\right\}. \quad (33)$$

where $z_i(i=1,2,...,8)$ signify the arbitrary constants.

6. Convergence Analysis

Initially idea of optimal homotopy analysis method is expressed by Liao [46, 47]. Mathematically it is given by

$$\varepsilon_m^f=\frac{1}{k+1}\Sigma_{i=0}^k\left[\aleph_f\left(\Sigma_{j=0}^m f(\eta)\right)_{\eta=i\delta^*\eta}\right]^2, \quad (34)$$

$$\varepsilon_m^\theta=\frac{1}{k+1}\Sigma_{i=0}^k\left[\aleph_\theta\left(\Sigma_{j=0}^m f(\eta),\Sigma_{j=0}^m\theta(\eta)\right)_{\eta=i\delta^*\eta}\right]^2, \quad (35)$$

$$\varepsilon_m^\phi=\frac{1}{k+1}\Sigma_{i=0}^k\left[\aleph_\phi\left(\Sigma_{j=0}^m f(\eta),\Sigma_{j=0}^m\theta(\eta),\Sigma_{j=0}^m\phi(\eta)\right)_{\eta=i\delta^*\eta}\right]^2, \quad (36)$$

Table 1. Shows Individual averaged squared residual errors.

m	ε_m^f	ε_m^θ	ε_m^ϕ
2	0.000229464	0.0000638014	0.0000869935
4	3.0261×10^{-6}	1.14194×10^{-8}	0.0000159683
8	1.47724×10^{-9}	1.259×10^{-10}	1.22628×10^{-6}
12	1.25034×10^{-12}	1.42071×10^{-13}	1.87871×10^{-7}
16	1.37702×10^{-15}	3.45887×10^{-16}	3.89476×10^{-8}
20	1.77366×10^{-18}	1.41566×10^{-18}	9.42204×10^{-9}

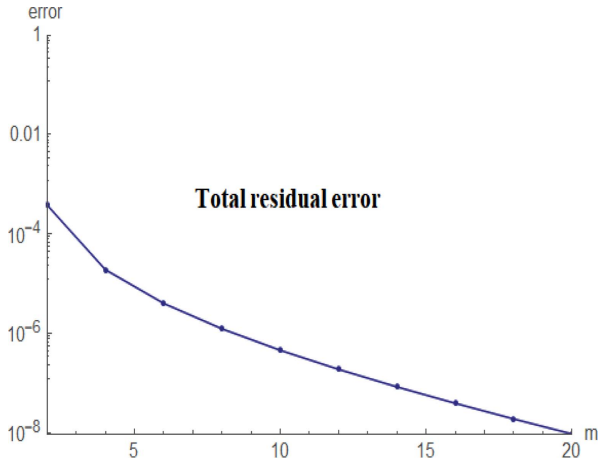

Fig. 2. (Color online) Total residual error.

Total squared residual error is [46, 47]:

$$\varepsilon_m^t = \varepsilon_m^f + \varepsilon_m^\theta + \varepsilon_m^\phi. \quad (40)$$

Total averaged squared residual error is highlighted in Fig. 2.

7. Graphical Results and Analysis

Physical description of various sundry variable on velocity, temperature distribution, entropy generation and concentration are deliberated.

7.1. Velocity

Fig. 3 is prepared to examine the impact of (A) on velocity. Physically an increment in curvature variable decays viscous force and therefore resistance in flow region is decreased. Thus velocity ($f'(\eta)$) is enhanced. Performance of velocity ($f'(\eta)$) with variation of magnetic parameter is depicted in Fig. 4. Larger magnetic parameter lead to improve the resistive force to liquid particles and as a result velocity of liquid decreased. An enhancement in velocity field ($f'(\eta)$) is noticed with variation of fluid parameter (see Fig. 5). Velocity ($f'(\eta)$) for melting parameter is shown in Fig 6. Higher melting parameter correspond to augments the velocity ($f'(\eta)$).

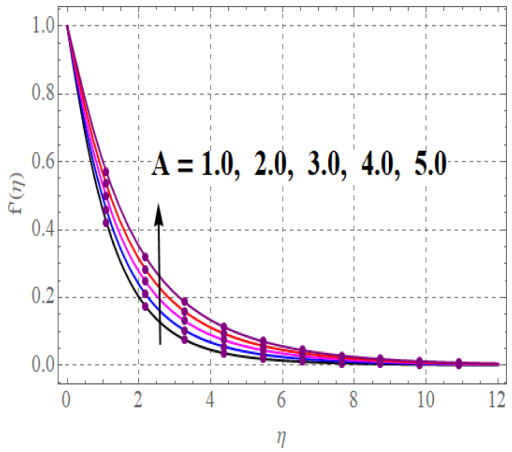

Fig. 3. (Color online) $f'(\eta)$ versus A.

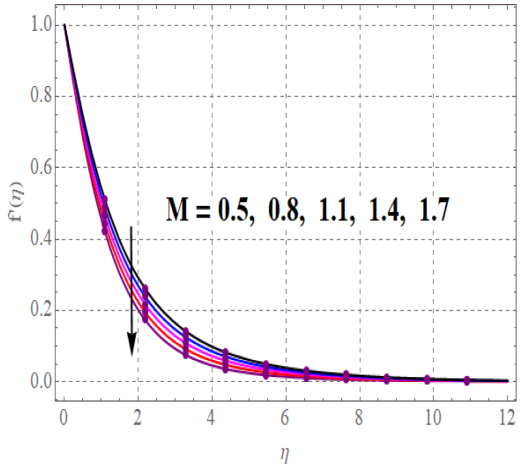

Fig. 4. (Color online) $f'(\eta)$ versus M.

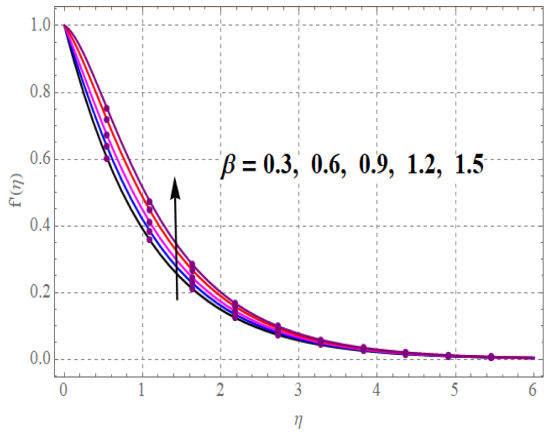

Fig. 5. (Color online) $f'(\eta)$ versus β_1.

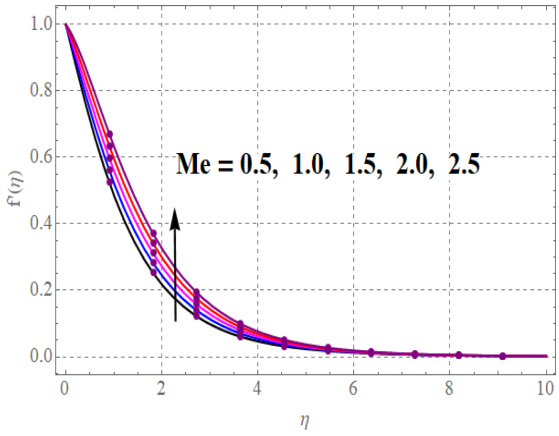

Fig. 6. (Color online) $f'(\eta)$ versus Me.

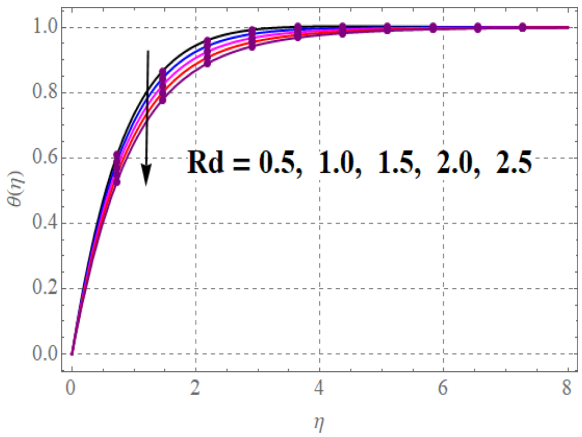

Fig. 7. (Color online) $\theta(\eta)$ versus Rd.

7.2. Temperature

Fig. 7 exhibits radiation parameter influence versus temperature distribution ($\theta(\eta)$). Clearly temperature distribution is reduced with variation of melting parameter.

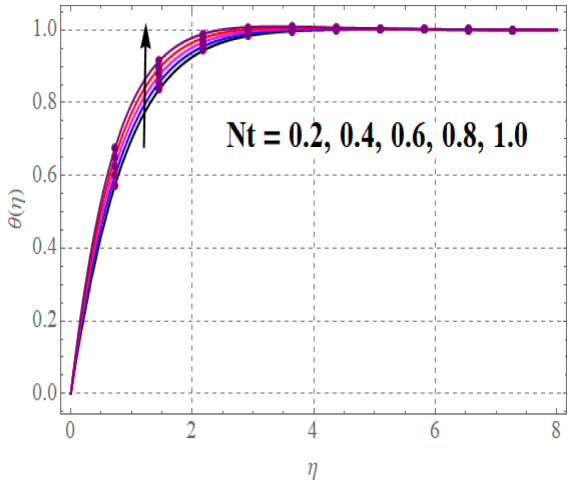

Fig. 8. (Color online) $\theta(\eta)$ versus Nt.

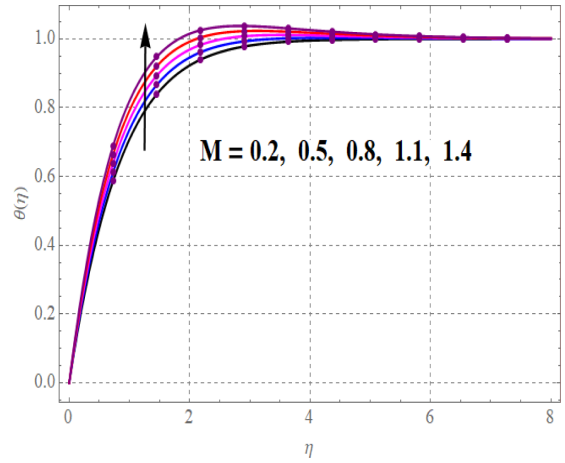

Fig. 9. θ(Color online) (η) versus M.

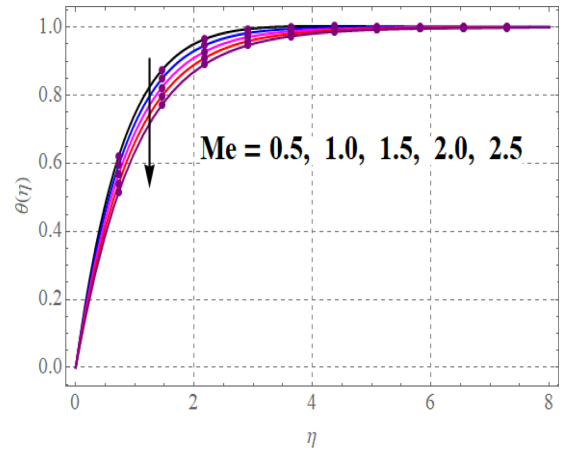

Fig. 10. (Color online) $\theta(\eta)$ versus Me.

An enhancement in thermophoresis variable (Nt) augments the temperature distribution (see Fig. 8). Outcomes of magnetic variable on temperature distribution ($\theta(\eta)$) is revealed in Fig. 9. In physical point of view, Lorentz force increases due to rising estimations of magnetic parameter, which is resistive force in nature (combination of electric and magnetic force on a point charge via electromagnetic fields) and as a results the diffusion rate inside the working material upsurge. That why the temperature distribution growths. Influence of melting parameter on temperature distribution ($\theta(\eta)$) is shown in Fig. 10. An enhancement in temperature ($\theta(\eta)$) is observed for melting parameter.

7.3. Concentration

Fig. 11 elucidates outcome of melting parameter on concentration ($\phi(\eta)$). Decay occurs in concentration ($\phi(\eta)$) versus melting parameter (Me). An opposite effect is noticed in concentration ($\phi(\eta)$) with variation of Brownian and thermophoresis diffusion parameters (Nt

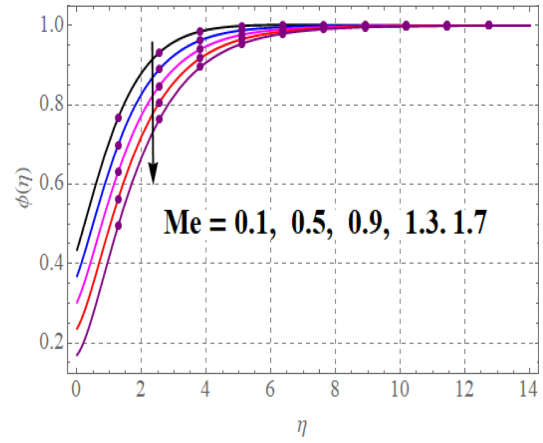

Fig. 11. (Color online) $\phi(\eta)$ versus Me.

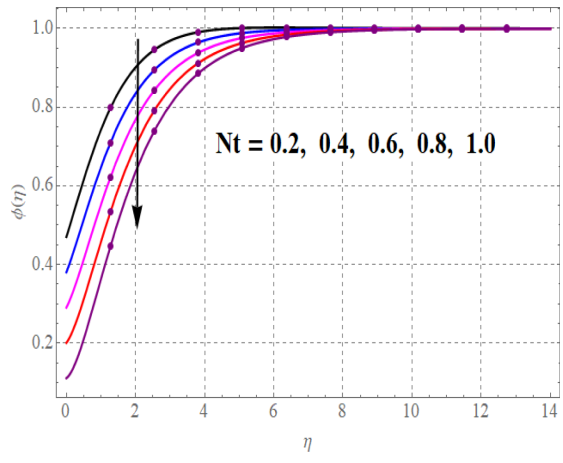

Fig. 12. (Color online) $\phi(\eta)$ versus Nt.

and *Nb*) (see Figs. 12 and 13). Outcomes of Schmidt number (*Sc*) on concentration is illustrated in Fig. 14. An augmentation in (*Sc*) leads to reduce mass diffusivity and thus concentration ($\phi(\eta)$) decreased.

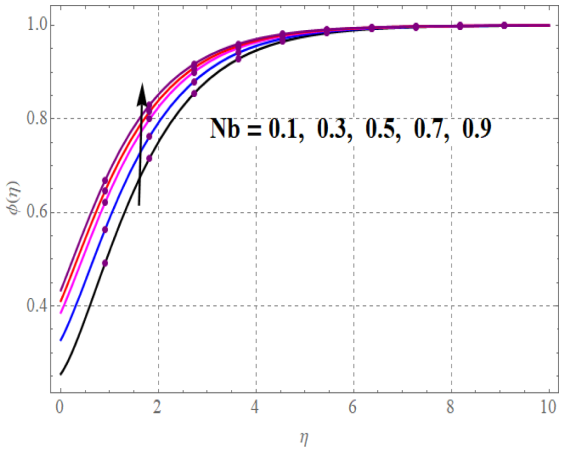

Fig. 13. (Color online) $\phi(\eta)$ versus Nb.

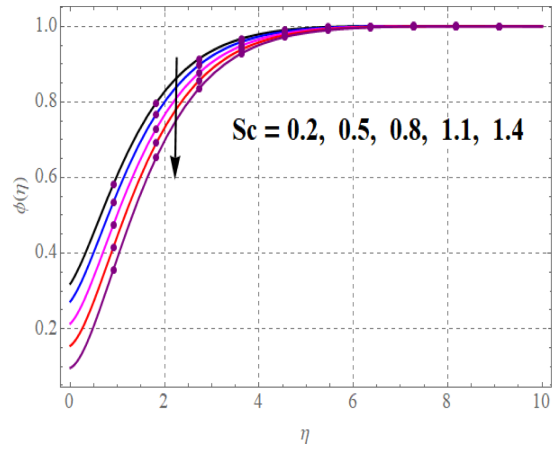

Fig. 14. (Color online) $\phi(\eta)$ versus Sc.

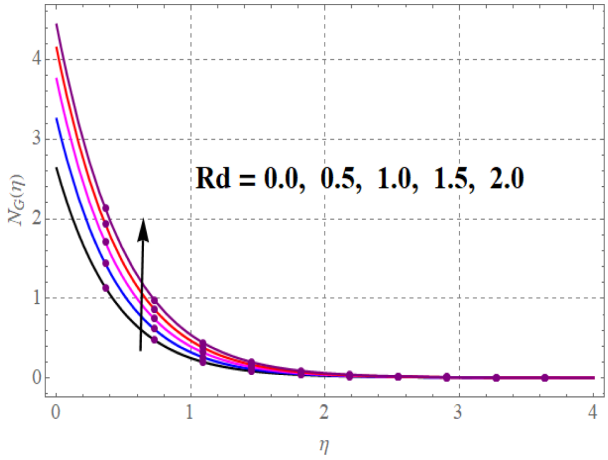

Fig. 15. (Color online) N_G versus Rd.

7.4. Entropy optimization

Fig. 15 elucidates variation of radiation parameter (*Rd*) on entropy generation (N_G). Physically an enhancement in radiation variable (*Rd*) leads to reduce mean absorption coefficient which augments emission of heat flux and consequently disorderness in thermal system rises. Therefore entropy generation (N_G) is boosted of an isolated

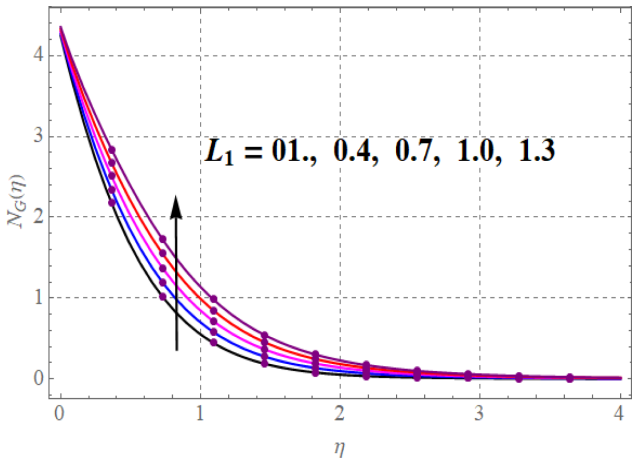

Fig. 16. (Color online) N_G versus L_1.

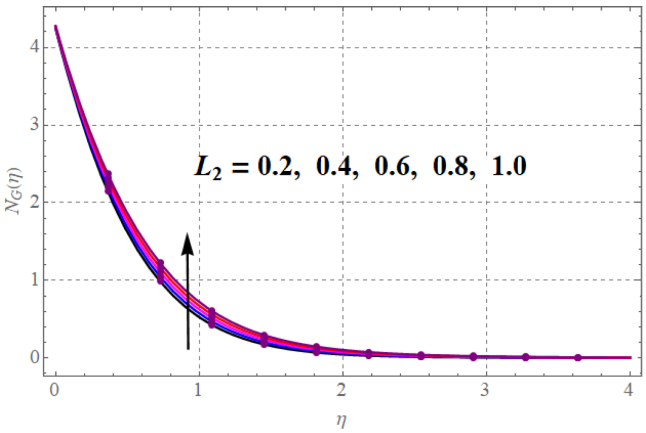

Fig. 17. (Color online) N_G versus L_2.

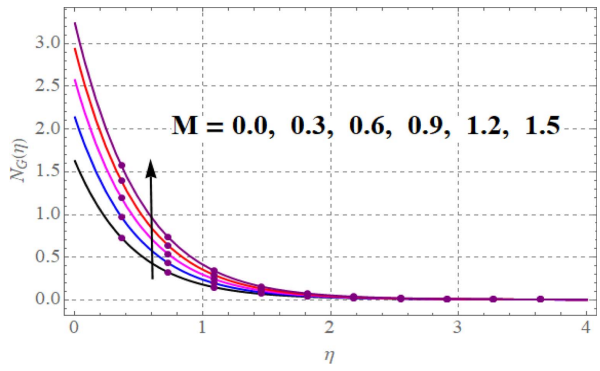

Fig. 18. (Color online) N_G versus *M*.

system. An augmentation in entropy generation (N_G) is observed for both diffusion parameters (see Figs. 16 and 7). Entropy generation (N_G) for magnetic variable is revealed in Fig. 18. Physically larger approximation of magnetic variable corresponds to rise the resistive force in the flow region and consequently collision amongst the particles. Therefore entropy optimization (N_G) is augmented.

8. Conclusions

The key observations are listed below.

- A reverse effect is noted for velocity field through magnetic and melting parameters.
- An augmentation in velocity field is observed for curvature parameter.
- Larger fluid parameter reduces the velocity.
- An opposite behavior is noticed for temperature and concentration versus thermophoresis parameter.
- A reduction occurs in temperature distribution for magnetic and melting parameters.
- An enhancement in temperature is observed for radiation.
- Concentration has reverse trend against melting parameter and Schmidt number.
- An increment in radiation variable improves the entropy generation.
- Entropy optimization is augmented versus diffusion parameters.
- An increment is observed for entropy rate through magnetic parameter.

Acknowledgement

The authors extend their appreciation to the Deanship of Scientific Research at King Khalid University, Abha 61413, Saudi Arabia for funding this work through research groups program under grant number GRP-18-1442.

Nomenclature

u, v : velocity components
r, s : curvilinear coordinates
T : temperature
T_m : melting heat temperature
T_∞ : ambient temperature
C_1 : homogeneous concentration
C_2 : heterogeneous concentration
C_0 : ambient concentration
A, B : chemical species
k_1^* : reaction rate (homogeneous species)
k_2^* : reaction rate (heterogeneous species)
p : pressure
α_1^* : material parameter
ρ_f : density
ν_f : kinematic viscosity
μ_f : dynamic viscosity
σ_f : electrical conductivity
k_f : thermal conductivity
c_p : specific heat
σ^* : Stefan Boltzmann constant
k^* : mean absorption coefficient
D_{C_1}, D_{C_2} : diffusion coefficients
D_T : thermophoresis coefficient
λ : latent heat
C_s : surface heat capacity
β : fluid parameter
M : magnetic parameter
Rd : radiation parameter
Pr : Prandtl number
Nt : thermophoresis parameter
Nb : Brownian motion parameter
Ec : Eckert number
Me : melting parameter
Sc : Schmidt number
K_1 : homogeneous reaction parameter
K_2 : heterogeneous reaction parameter
δ : diffusivity ratio
C_{fs} : surface drag force
τ_{rs} : shear stress
Nu_s : Nusselt number
q_w : heat flux
Re_s : local Reynold number
N_G : entropy generation
Br : Brinkman number
α_1 : temperature difference parameter
L_1 : homogeneous diffusion parameter
L_2 : heterogeneous diffusion parameter

References

[1] P. Zhang, Z. N. Meng, H. Zhu, Y. L. Wang, and S. P. Peng, Applied Energy **185**, 1971 (2017).
[2] L. Roberts, Journal of Fluid Mechanics **4**, 505 (1958).
[3] F. Mabood and A. Mastroberardino, Journal of the Taiwan Institute of Chemical Engineers **57**, 62 (2015).
[4] B. Gurel, International Journal of Heat and Mass Transfer **148**, 119117 (2020).
[5] T. Hayat, M. Imtiaz, and A. Alsaedi, Advanced Powder Technology **27**, 1301 (2016).
[6] M. R. Krishnamurthy, B. C. Prasannakumara, B. J. Gireesha, and R. S. R. Gorla, Engineering Science and Technology, an International Journal **19**, 53(2016).

[7] M. Sheikholeslami and H. B. Rokni, International Journal of Heat and Mass Transfer **114**, 517 (2017).
[8] M. I. Khan, S. Qayyum, T. Hayat, M. I. Khan, and A. Alsaedi, International Journal of Heat and Mass Transfer **133**, 959 (2019).
[9] T. Hayat, S. A. Khan, M. I. Khan, and A. Alsaedi, Physica Scripta **94**, 085001 (2019).
[10] M. A. A. Mahmoud and S. E. Waheed, Applied Mathematics and Mechanics **35**, 979 (2014).
[11] T. Hayat, M. I. Khan, M. Tamoor, M. Waqas, and A. Alsaedi, Results in Physics **7**, 1824 (2017).
[12] N. V. Ganesh, Q. M. Al-Mdallal, and P. K. Kameswaran, Case Studies in Thermal Engineering **13** 100413 (2019).
[13] T. Chakraborty, K. Das, and P. K. Kundu, Journal of Molecular Liquids **229**, 443 (2017).
[14] T. Hayat, N. Aslam, M. I. Khan, M. I. Khan, and A. Alsaedi, Journal of Molecular Liquids **275**, 599 (2019).
[15] B. J. Gireesha, G. Sowmya, M. I. Khan, and H. F. Öztop, Computer Methods and Programs in Biomedicine **185**, 105166 (2020).
[16] N. Bachok, A. Ishak, and I. Pop, Physics Letters A **374**, 4075 (2010).
[17] N. Mally and S. Haussener, International Journal of Heat and Mass Transfer **164** 120525, (2021).
[18] R. Qi, Z. Wang, J. Ren, and Y. Wu, International Journal of Heat and Mass Transfer **157**, 119927 (2020).
[19] M. I. Khan, A. Alsaedi, T. Hayat, and N. B. Khan, Computer Methods and Programs in Biomedicine **179**, 104973 (2019).
[20] S. A. M. Mehryan, M. Vaezi, M. Sheremet, and M. Ghalambaz, International Journal of Heat and Mass Transfer **151**, 119385 (2020).
[21] S. U. S. Choi and J. A. Eastman, ASME Publications-Fed **231**, 99 (1995).
[22] J. A. Eastman, S. U. S. Choi, S. Li, W. Yu, and L. J. Thompson, Applied Physics Letters **78**, 718 (2001).
[23] J. Buongiorno, Journal of Heat Transfer **128**, 240 (2006).
[24] S. A. Khan, T. Hayat, and A. Alsaedi, International Communications in Heat and Mass Transfer **119**, 104890 (2020).
[25] I. Ullah, S. Shafie, I. Khan. and K. L. Hsiao, Results in Physics **9**, 183 (2018).
[26] G. Kumaran and N. Sandeep, Journal of Molecular Liquids **233**, 262 (2017).
[27] Y. Lin and Y. Jiang, International Journal of Heat and Mass Transfer **123**, 569 (2018).
[28] M. I. Khan, S. A. Khan, T. Hayat, M. I. Khan, and A. Alsaedi, Computer Methods and Programs in Biomedicine **180**, 105017 (2019).
[29] T. Tsuji, S. Saita, and S. Kawano, Physica A: Statistical Mechanics and its Applications **493**, 467 (2018).
[30] M. A. Sheremet, D. S. Cimpean, and I. Pop, Applied Thermal Engineering **113**, 413 (2017).
[31] S. E. Ghasemi, Journal of Molecular Liquids **238**, 115 (2017).
[32] A. Bejan, Journal of Applied Physics **79**, 1191 (1996).
[33] A. Bejan, Energy **5**, 721 (1980).
[34] T. Hayat, S. A. Khan, M. I. Khan, and A. Alsaedi, Computer Methods and Programs in Biomedicine **177**, 57 (2019).
[35] S. Haider, A. S. Butt, Y. Li, S.M. Imran, B. Ahmad, and A. Tayyaba, Symmetry **12**, 1 (2020).
[36] Z. Zhang, C. Lou, Z. Li, and Y. Long, Journal of Quantitative Spectroscopy and Radiative Transfer **253**, 107175 (2020).
[37] M. Torabi, N. Karimi, M. Torabi, G. P. Peterson, and J. Carey, International Journal of Heat and Mass Transfer **163**, 120471 (2020).
[38] L. H. K. Goh, Y. M. Hung, G. M. Chen, and C. P. Tso, International Journal of Thermal Sciences **160**, 120471, (2021).
[39] M. A. Vatanparast, S. Hossainpour, A. K. Asl, and S. Forouzi, International Communications in Heat and Mass Transfer **111**, 104446 (2020).
[40] S. E. Ahmed, M. A. Mansour, A. Mahdy, and S. S. Mohamed, Engineering Science and Technology, an International Journal **20**, 1553 (2017).
[41] Z. Zhang, C. Lou, Z. Li, and Y. Long, Journal of Quantitative Spectroscopy and Radiative Transfer **253**, 107175 (2020).
[42] M. M. Ghorani, M. H. S. Haghighi, A. Maleki, and A. Riasi, Renewable Energy **162**, 1036 (2020).
[43] M. Waqas, M. I. Khan, T. Hayat, M. M. Gulzar, and A. Alsaedi, Chaos, Solitons & Fractals **130**, 109415 (2020).
[44] M. I. Khan and F. Alzahrani, Journal of Theoretical and Computational Chemistry **19**, 2040006 (2020).
[45] M. I. Khan, F. Alzahrani, A. Hobiny, and Z. Ali, Journal of Materials Research and Technology **9**, 6172 (2020).
[46] S. J. Liao, Springer, Heidelberg, Germany (2012).
[47] S. J. Liao, Communications in Nonlinear Science and Numerical Simulation **15** 2003 (2010).
[48] T. Hayat, A. Shafiq, and A. Alsaedi, Journal of Magnetism and Magnetic Materials **405**, 97 (2016).
[49] M. Sheikholeslami, M. Hatami, and D. D. Ganji, Journal of Molecular Liquids **194**, 30 (2014).
[50] S. Han, L. Zheng, C. Li, and X. Zhang, Applied Mathematics Letters **38**, 87 (2014).
[51] I. L. Animasaun, B. Mahanthesh, G. Sarojamma, and J. S. Damisa, Physica A: Statistical Mechanics and its Applications **549**, 124047 (2020).
[52] R. Kumar, R. Kumar, M. Sheikholeslami, and A. J. Chamkha, Journal of Molecular Liquids **274**, 379 (2019).
[53] O. D. Makinde and I. L. Animasaun, Journal of Molecular Liquids **221**, 733 (2016).
[54] I. L. Animasaun, Alexandria Engineering Journal **55**, 2375 (2016).
[55] R. S. Saif, T. Muhammad, H. Sadia, and R. Ellahi, Physica A: Statistical Mechanics and its Applications **551**, 124060 (2020).
[56] M. I. Khan and F. Alzahrani, Mathematics and Computers in Simulation **185**, 47 (2021).
[57] T. Hayat, F. Shah, and A. Alseadi, International Communications in Heat and Mass Transfer **119**, 104824 (2020).